



This is a repository copy of *Accelerated carbonation testing of alkali-activated slag/metakaolin blended concretes: effect of exposure conditions.*

White Rose Research Online URL for this paper:
<http://eprints.whiterose.ac.uk/97159/>

Version: Accepted Version

Article:

Bernal, S.A., Provis, J.L. orcid.org/0000-0003-3372-8922, Mejia de Gutierrez, R. et al. (1 more author) (2015) Accelerated carbonation testing of alkali-activated slag/metakaolin blended concretes: effect of exposure conditions. *Materials and Structures*, 48 (3). pp. 653-669. ISSN 1359-5997

<https://doi.org/10.1617/s11527-014-0289-4>

Reuse

Unless indicated otherwise, fulltext items are protected by copyright with all rights reserved. The copyright exception in section 29 of the Copyright, Designs and Patents Act 1988 allows the making of a single copy solely for the purpose of non-commercial research or private study within the limits of fair dealing. The publisher or other rights-holder may allow further reproduction and re-use of this version - refer to the White Rose Research Online record for this item. Where records identify the publisher as the copyright holder, users can verify any specific terms of use on the publisher's website.

Takedown

If you consider content in White Rose Research Online to be in breach of UK law, please notify us by emailing eprints@whiterose.ac.uk including the URL of the record and the reason for the withdrawal request.



eprints@whiterose.ac.uk
<https://eprints.whiterose.ac.uk/>

Accelerated carbonation testing of alkali-activated slag/metakaolin blended concretes: effect of exposure conditions

Susan A. Bernal,^{1,2} John L. Provis,^{2*} Ruby Mejía de Gutiérrez,¹ Jannie S.J. van Deventer^{3,4}

¹School of Materials Engineering, Composite Materials Group, CENM, Universidad del Valle, Cali, Colombia

²(current address) Department of Materials Science and Engineering, University of Sheffield, Sir Robert Hadfield Building, Mappin St, Sheffield S1 3JD, United Kingdom

³Zeobond Pty Ltd, P.O. Box 210, Somerton, Victoria 3062, Australia

⁴Department of Chemical and Biomolecular Engineering, University of Melbourne, Victoria 3010, Australia

* To whom correspondence should be addressed. Email j.provis@sheffield.ac.uk, phone +44 114 222 5490, fax +44 114 222 5943

Abstract

This paper addresses the effects of relative humidity and CO₂ concentration on the rate and effects of accelerated carbonation in alkali-activated slag/metakaolin concretes. Strength and water absorption are used alongside phenolphthalein measurements to monitor carbonation, and the effects of drying at different relative humidities are particularly significant in controlling carbonation rates. Different trends in the carbonation rate as a function of metakaolin content are observed when varying the CO₂ concentration, further revealing that the carbonation rates of these materials under accelerated conditions are influenced strongly by the testing protocol. The standard phenolphthalein method for testing carbonation depth appears only to be capturing the change in alkalinity with pore solution carbonation, meaning that it does not correlate well with other performance parameters at high CO₂ concentrations.

Keywords: alkali-activated cement; concrete; granulated blast-furnace slag; carbonation; durability

1. Introduction

Durability of structures and structural concretes, particularly in the presence of aggressive agents, is a topic of fundamental interest and importance in civil infrastructure and construction. Carbon dioxide

36 (CO₂) is particularly known to affect the durability of cement-based materials under long-term
37 exposure, through a degradation process referred to as carbonation [1-3]. This phenomenon is
38 controlled by both gas diffusion and chemical reaction mechanisms, and consequently its progress is
39 determined by both the chemistry of the binder and the permeability of the material. The effect of
40 carbonation in concrete structures is a reduction in the alkalinity of the material, leading to an
41 increased susceptibility to corrosion of embedded steel reinforcement, often accompanied by a
42 decrease in mechanical strength [2, 4, 5].

43
44 Carbonation of mortars and concretes produced using ordinary Portland cement has been widely
45 studied. In these systems, the CO₂ from the atmosphere diffuses through gas-filled pores and dissolves
46 in the pore solution to form aqueous HCO₃⁻. This uptake of acidic CO₂ into the alkaline pore solution
47 reduces the internal pH of the binder, and the dissolved carbonate also reacts with the calcium-rich
48 hydration products present in the matrix, mainly with the portlandite (Ca(OH)₂), calcium silicate
49 hydrate (C-S-H) and calcium aluminate hydrate phases, to form solid calcium carbonates [4, 6, 7]. In
50 Portland cement-based systems, it is well known that the progress of carbonation is dependent on the
51 chemical nature of the binder phases with which the CO₂ is going to react, as well as the factors
52 determining the diffusion rate of the gaseous CO₂, such as the pore network and exposure
53 environment, in particular relative humidity [8-11]. It has been reported [9] that carbonation is more
54 rapid at intermediate relative humidity (50–70%), and this is attributed to interactions between drying
55 and carbonation processes [12], as the presence of a very high fraction of pores filled with water
56 hinders the diffusion of CO₂, while sufficient water is required to promote the solvation and hydration
57 of the carbon dioxide. Under intermediate moisture conditions both reaction kinetics and diffusion of
58 CO₂ are favoured, which leads to acceleration of the carbonation process [4].

59
60 In the case of concretes based on alkali-activated binders, there is limited existing knowledge about
61 the long-term in-service stability of these materials, although the studies that have been published
62 show generally moderate to low carbonation rates (<0.5 mm/yr), similar to the carbonation rate of
63 Portland cement concretes, under service conditions in continental climates [13-15]. Shi, Krivenko
64 and Roy report the natural carbonation rates of concrete structures with ages between 12 and 40 years,
65 located in Russia, Ukraine and Poland [14]. The concretes were produced from alkali-activated slag,
66 using alkaline activator solutions of sodium metasilicate, sodium carbonate and potassium carbonate,
67 and had 28-day compressive strengths between 35 - 82 MPa. The in-service carbonation rates,
68 measured using the phenolphthalein method, did not exceed 1 mm/year in any of the cases described.
69 Similar results were identified in 7-year-old silicate-activated slag concretes [16], where the
70 carbonated depths identified were much lower than would be predicted through calculations based on

71 accelerated carbonation testing, demonstrating that the exposure conditions used in accelerated testing
72 do not replicate the phenomena that take place under natural service conditions.

73
74 On the other hand, laboratory studies of pastes and mortars of alkali-activated slag, and
75 slag/metakaolin blends [15, 17-21], have indicated high susceptibility to carbonation in these
76 materials under accelerated conditions, compared with conventional cements. It is proposed that this
77 is due particularly to effects related to pore solution alkalinity [22] and binder chemistry, especially
78 the absence of portlandite as a reaction product in these binders. More recently it has been identified
79 [23] that drying of alkali-activated materials induces changes in their microstructure. This causes
80 severe microcracking, which is deleterious when pre-conditioning specimens prior to analysis of
81 water absorption properties and accelerated carbonation testing. Considering these observations, it is
82 evident that there is the need to develop a better understanding of the real meaning of the results
83 obtained in alkali-activated materials, and how accelerated carbonation tests should be conducted, as
84 the divergences between accelerated and natural carbonation rates of alkali-activated concretes are
85 remarkable [16].

86
87 The carbonation of concrete under ambient conditions is generally relatively slow, as a consequence
88 of the relatively low concentration of CO₂ in the atmosphere (0.03 – 0.04%). This has led to the
89 development of experimental methods based on accelerated carbonation under controlled conditions,
90 through exposure to high CO₂ concentrations for shorter periods of time. It has been noted [24] that a
91 short period of accelerated carbonation in Portland cement-based materials is not necessarily directly
92 analogous to long term exposure to natural atmosphere, which involves differences in moisture
93 distribution under different drying periods, and gradual changes in the micropore structure due to
94 ageing and carbonation. A proposed European standard method [25] for testing the susceptibility of
95 Portland cement-based materials to carbonation has been discussed in detail by Harrison et al. [26],
96 and adopted recently by some nations, but not in general across the EU [26]. Some limitations of
97 common accelerated test methods, such as repeatability and reproducibility, have also been identified,
98 even in application to Portland cement-based systems [27, 28].

99
100 For the specific case of alkali-activated binders, recent results [22] reveal that the mechanism of
101 carbonation in alkali activated slag which is induced using accelerated test methods is strongly
102 affected by the CO₂ concentration, leading to differences in the chemistry of the alkali carbonate
103 phases formed as a result of carbonation, and also the pH and carbonate/bicarbonate ratio of the
104 remaining pore solution. This will therefore change both the CO₂ uptake rate and the influence of the
105 carbonated pore solution on steel corrosion chemistry, meaning that the test results must be carefully
106 interpreted in order to give an accurate prediction of either the rate or the effects of carbonation in
107 these materials under natural conditions. In particular, it appears from thermodynamic calculations

108 related to pore solution chemistry [22] that accelerated testing will overestimate both the rate and
109 degradation effects of carbonation in alkali-activated binders. From these results, it seems likely that
110 if an alkali-activated concrete and a Portland cement concrete show the same carbonation depth in an
111 accelerated test, the alkali-activated material will suffer less carbonation under natural conditions, and
112 thus the service life would be much higher. However, further detailed experimental work related to
113 understanding the effects induced by different accelerated testing conditions is undoubtedly required
114 before such statements can be fully validated.

115

116 This indicates that the exposure conditions which are used to induce accelerated carbonation of alkali-
117 activated materials need to be studied, in order to provide recommendations for appropriate testing
118 protocols, and also to aid in interpretation of the results obtained. The aim of this study is therefore to
119 assess the effects of relative humidity and CO₂ concentration on the carbonation rate of alkali-
120 activated concretes during accelerated testing. The concretes tested have a binder based on a
121 combination of granulated blast furnace slag (GBFS) and metakaolin (MK), activated by sodium
122 silicate solutions, where the addition of the metakaolin serves to regulate the setting of these materials
123 which are based on an otherwise very rapidly-reacting slag, and also enhances strength when the
124 activator dose is sufficient [29, 30]. In addition to carbonation depth measurements, variations in
125 mechanical strength and pore network properties, investigated in an indirect way via water absorption
126 tests, are monitored during CO₂ exposure, to obtain a deeper understanding of the microstructural
127 changes in the concretes which are induced under different exposure conditions.

128

129

130

131 **2. Materials and methods**

132

133 **2.1. Materials**

134

135 The primary raw material used in this study was a Colombian granulated blast furnace slag (GBFS)
136 from the factory Acerías Paz del Río. Its specific gravity was 2900 kg/m³ and Blaine fineness was 399
137 m²/kg. The particle size range, determined through laser granulometry, was 0.1–74 µm, with a d₅₀ of
138 15 µm. The metakaolin (MK) used was generated in the laboratory by calcination of a kaolin
139 containing minor quartz and dickite impurities [29]. Calcination was carried out at 700°C in an air
140 atmosphere, for 2 h. The particle size range of the MK was 1.8–100 µm, with a d₅₀ of 13.2 µm and
141 10% of particles finer than 4 µm.

142

143 **Table 1.** Compositions of the MK and GBFS used, from X-ray fluorescence analysis. LOI is loss on
144 ignition at 1000°C

Raw material	Component (mass % as oxide)							LOI
	SiO ₂	Al ₂ O ₃	CaO	Fe ₂ O ₃	MgO	TiO ₂	Others	
GBFS	32.29	16.25	42.45	2.35	2.87	0.50	0.57	2.72
MK	50.72	44.63	2.69	-	-	-	0.94	1.02

145

146 Alkaline activating solutions were formulated by blending a commercial sodium silicate solution
147 (32.4 wt.% SiO₂, 13.5 wt.% Na₂O and 54.1 wt.% H₂O), and 50 wt.% NaOH solution, with the slag
148 and metakaolin, to reach the desired overall molar ratios (specified as SiO₂/Al₂O₃ (S/A)), and
149 corresponding to a concentration of activation of 11-12% Na₂O relative to the amount of binder (i.e.,
150 11-12 g Na₂O per 100 g GBFS+MK).

151

152 Crushed gravel and river sand were used as coarse and fine aggregates. The coarse aggregate was of
153 19 mm maximum size, with a specific gravity of 2790 kg/m³ and absorption of 1.23%. The specific
154 gravity, absorption, and fineness modulus of the sand were 2450 kg/m³, 3.75% and 2.57, respectively.

155

156 2.2. Concrete mixes

157

158 The concretes were produced with total binder (GBFS+MK) contents of 400 kg/m³ and a total
159 water/(GBFS+MK+anhydrous activator) ratio of 0.47. Fresh concrete was mixed, poured into
160 cylindrical steel moulds ($\phi = 76.2$ mm, $h = 152.4$ mm), tamped and levelled. The concrete specimens
161 were then cured in a humidity-controlled chamber at 25±5°C and 90% relative humidity (RH), for 28
162 days, with the moulds removed after 24 hours. The mix designs are given in Table 2. Detailed
163 analysis of the evolution of engineering (compressive and flexural strength) and durability properties
164 (water absorption properties, chloride permeability and carbonation) of the concrete mixes assessed in
165 this study as a function of the time of curing is reported in [30].

166

167 **Table 2.** Mix designs of the concretes. All quantities are in kg/m³ of fresh concrete

Component	GBFS/(GBFS+MK)		
	1.0	0.9	0.8
GBFS	400	360	320
MK	-	40	80
Sodium silicate solution	120	136	132
NaOH (50 wt.% solution)	68	72	78
Coarse aggregate	832	816	808
Sand	832	816	808
Free water	132	124	124
Overall SiO ₂ /Al ₂ O ₃ molar ratio	4.4	4.0	3.6
Activator concentration	10.6	11.6	12.0

(% Na₂O by mass of
GBFS + MK)

168

169

170 **2.3. Accelerated carbonation testing**

171

172 After 28 days of curing the specimens were removed from the humidity chamber, and then the top
173 ends of the specimens were covered using an acrylic resin (Acronal ®), applying a minimum of 4
174 layers, to direct the ingress of CO₂ through the curved face of the cylinders during testing. Samples
175 were then transferred to the carbonation chamber for CO₂ exposure, without application of an
176 intermediate drying or conditioning step. This was done to minimise any potential microcracking or
177 differences in sample maturity which would be observed if they were conditioned for extended
178 periods at the testing relative humidity, a step which is specified in many testing protocols for
179 Portland cement systems.

180

181 2.3.1. Variation of relative humidity

182

183 An accelerated carbonation testing system with automated control of temperature, humidity and CO₂
184 concentration was used to induce the carbonation of concrete specimens. A CO₂ concentration of 1.0
185 ± 0.2%, was used, at a temperature of 25 ± 2 °C, and RH values of 50 ± 5%, 65 ± 5%, and 80 ± 5%,
186 where the uncertainties quoted here are the maximum allowable deviations from setpoints as specified
187 by the supplier of the chamber control systems. Specimens were removed from the chamber after 250
188 or 500 h of exposure, and the depth of carbonation was measured by treating the surface of a freshly
189 cleaved specimen with a 1% solution of phenolphthalein in alcohol. In the uncarbonated part of the
190 specimen, where the concrete was still highly alkaline, purple-red colouration was obtained, while
191 there was no colour change observed in the carbonated region. Each result is reported as the average
192 depth of carbonation measured at eight points, using two replicate samples (four points per sample;
193 the standard deviation of each carbonation depth measurement is similar to or smaller than the size of
194 the points on the graphs as plotted). The properties of uncarbonated samples after 28 days of curing
195 are used as reference values, indicated as zero hours of exposure.

196

197 2.3.2. Variation of CO₂ exposure concentration

198

199 Specimens were exposed to CO₂ concentrations of 1 ± 0.2% and 3.0 ± 0.2%, at a relative humidity of
200 65 ± 5%. After 250, 500, 750 and 1000 h of exposure, carbonation depths were determined as
201 described above.

202

203 **2.4. Testing protocols**

204

205 Carbonated and uncarbonated concretes were tested for compressive strength following the standard
206 procedure ASTM C39/C39M-09a (Standard Test Method for Compressive Strength of Cylindrical
207 Concrete Specimens). Total porosity and absorption were determined before and after carbonation
208 according to the standard procedure ASTM C642-06 (Standard Test Method for Density, Absorption,
209 and Voids in Hardened Concrete), where the samples are dried and then boiled in water to determine
210 the total volume of permeable voids. Capillary sorptivity was assessed by applying the standard
211 procedure EMPA–SIA 162/1 [31], in which water is allowed to pass from a damp sponge into a dried
212 cylindrical sample through a process of capillary suction, and the mass of the sample is monitored as a
213 function of time.

214

215 **3. Results and discussion**

216

217 **3.1. Effect of relative humidity on the accelerated carbonation of alkali-activated GBFS/MK**
218 **blends**

219

220 3.1.1. Carbonation rate

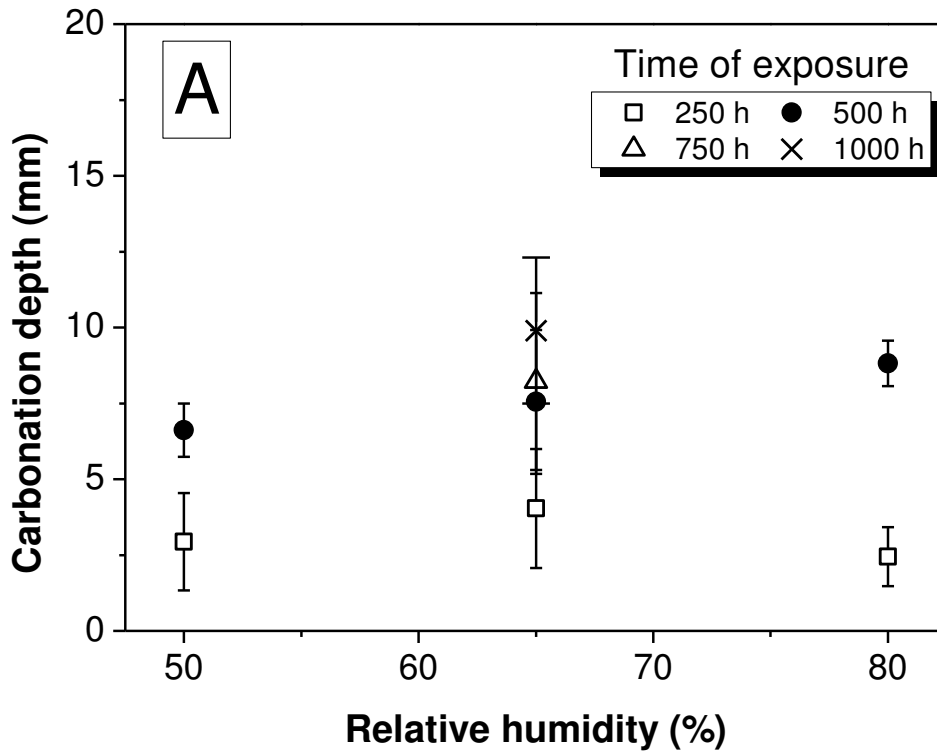
221

222 Figure 1 shows the carbonation depth as a function of time and relative humidity for the samples
223 containing different percentages of metakaolin. There are two clearly distinct types of behaviour
224 shown by the samples when considering carbonation as a function of time:

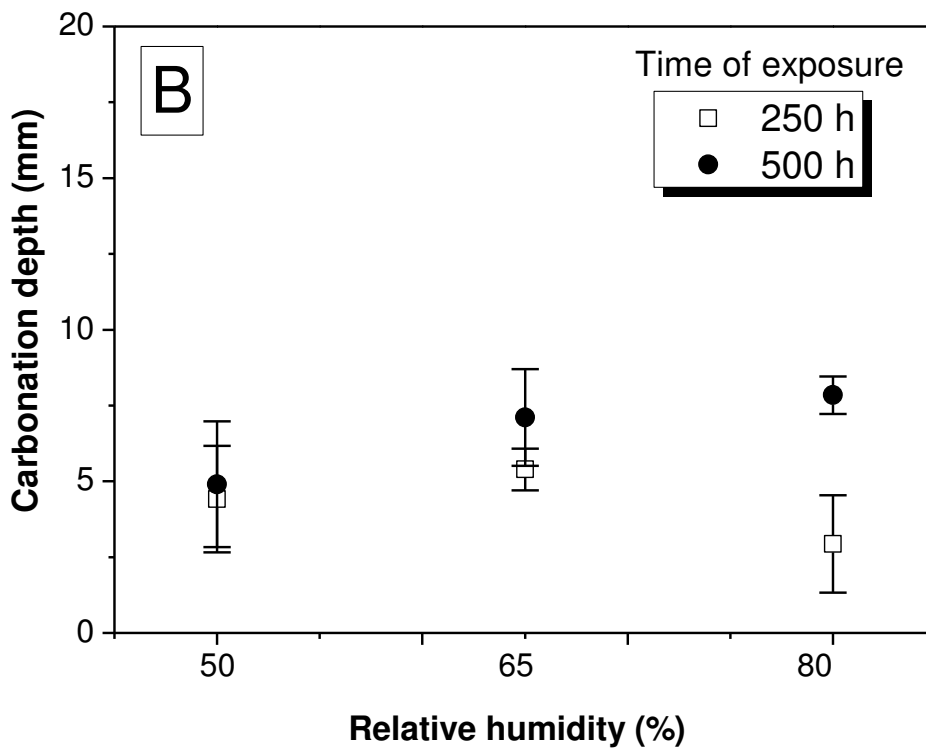
- 225 - All of the GBFS-only samples, and the sample with $\text{GBFS}/(\text{GBFS}+\text{MK}) = 0.9$ exposed at 80%
226 RH, show relatively slow initial carbonation, but then the ingress of the carbonation front
227 accelerates, and the increment in carbonation depth from 250-500 h is more than the carbonation
228 observed in the first 250 h
- 229 - All of the samples with $\text{GBFS}/(\text{GBFS}+\text{MK}) = 0.8$, and the samples with $\text{GBFS}/(\text{GBFS}+\text{MK}) = 0.9$
230 exposed at 50 and 65% RH, show a deceleration in carbonation with time, with more carbonation
231 in the first 250 h than in the subsequent 250 h.

232

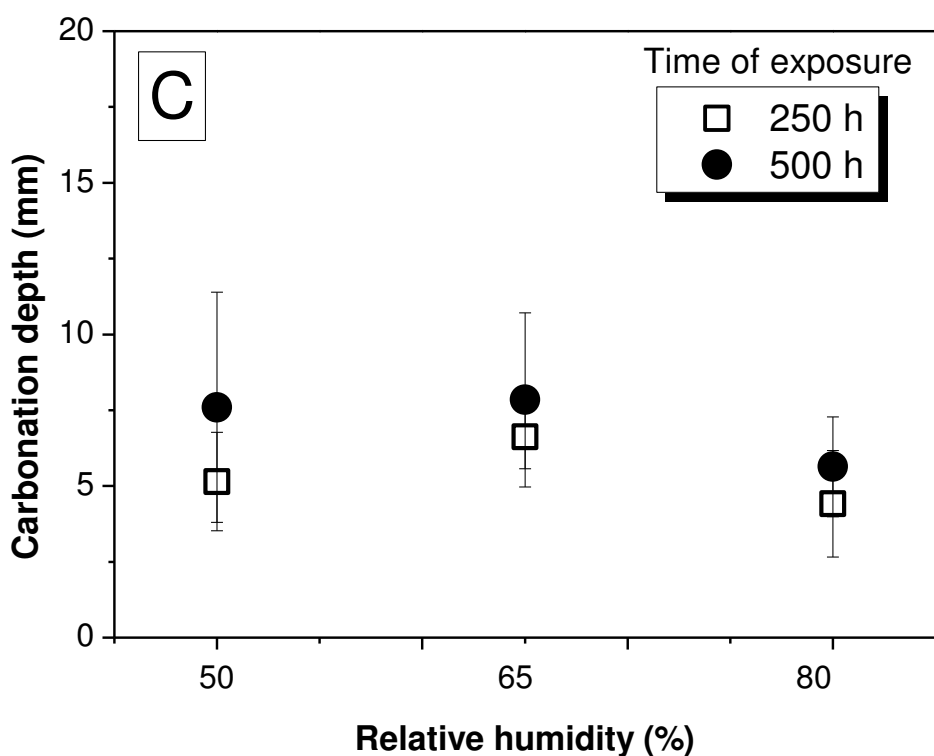
233



234



235



236

237 **Figure 1.** Carbonation depth as a function of the relative humidity and time of exposure in alkali-
238 activated GBFS/MK concretes, formulated with GBFS/(GBFS+MK) ratios of (A) 1.0, (B) 0.9 and (C)
239 0.8, at 1% CO₂. Error bars show ± 1 standard deviation among 5 measurements per sample.

240

241 Figure 1 also shows differences in the trend in carbonation depth as a function of relative humidity,
242 depending on the binder composition and the exposure time. In specimens solely based on GBFS
243 (Figure 1A) similar carbonation depths are identified at each different RH during the first 250 h of
244 exposure, and the carbonation depth increases with RH after 500 h of CO₂ exposure. A similar trend is
245 observed in specimens with GBFS/(GBFS+MK) = 0.9, although the carbonation rate within the first
246 250 h at 80% RH is notably lower than at the other relative humidities studied. Similar results are
247 observed at higher content of MK in the binder (GBFS/(GBFS+MK) = 0.8, Figure 1C) with the most
248 rapid carbonation observed at intermediate humidity.

249

250 The acceleration in carbonation of some of the concretes (Figure 1A,B) between the first 250 h and
251 the subsequent 250 h of curing is to some extent counterintuitive; such a change in kinetics would not
252 be expected if the process were simply controlled by either diffusion or chemical reaction
253 mechanisms [32, 33]. Even if the microstructural damage associated with the carbonation-induced
254 decalcification of the C-A-S-H gel to form calcium carbonate products [17] was so severe that the
255 damaged material did not provide any barrier to CO₂ diffusion, this would result in a linear rate of

256 carbonation, but could not explain an acceleration in rate. There must therefore be a combination of
257 drying and carbonation effects which leads to this apparent acceleration during this timeframe. There
258 is only one dataset available (Figure 1A) which contains data at 750 and 1000 h for a sample which
259 showed an acceleration effect; these data show that the carbonation decelerated again after 500 h,
260 which is consistent with the development of some extent of diffusional resistance to mass transport in
261 the later stages of carbonation, as would be expected from the thickness of the carbonated layers on
262 the samples.

263

264 The higher final extent of carbonation at higher relative humidities is consistent with the trends
265 reported for Portland cement concretes containing supplementary cementitious materials [34, 35],
266 where it is expected that the presence of water-saturated pores will hinder the diffusion of CO₂
267 through the material. Partially water-filled pores are known to accelerate carbonation through
268 convective mass transport, and also by providing high interfacial areas for transfer of CO₂ from gas to
269 liquid (and thus subsequently to solid) phases [9, 11]. For the GBFS-only samples, which have the
270 lowest water absorption in the uncarbonated state [30], and for the GBFS/(GBFS+MK) = 0.9 sample
271 at high (80%) relative humidity, it is likely that the pores are more extensively filled with water, so
272 the start of carbonation is slowed after the drying front has begun to enter the sample. The higher
273 water absorption measured for the uncarbonated GBFS/(GBFS+MK) = 0.8 samples [30] indicates that
274 there are already unsaturated pores within the concrete prior to the start of the carbonation tests for
275 these concretes, and the observed carbonation behaviour does not show an acceleration event.

276

277 Comparing the samples with different MK contents, it appears that when concretes are exposed under
278 comparable relative humidity conditions for 500 h, increased metakaolin content will usually give a
279 lower extent of carbonation. The only exception to this trend in Figure 1 is the sample with
280 GBFS/(GBFS+MK) = 0.8 at 50% RH, which is more rapidly carbonated than the sample with
281 GBFS/(GBFS+MK) = 0.9 under the same conditions. It is likely that this is related to the higher
282 porosity of the concretes with GBFS/(GBFS+MK) = 0.8 [30], as will be discussed in detail below.

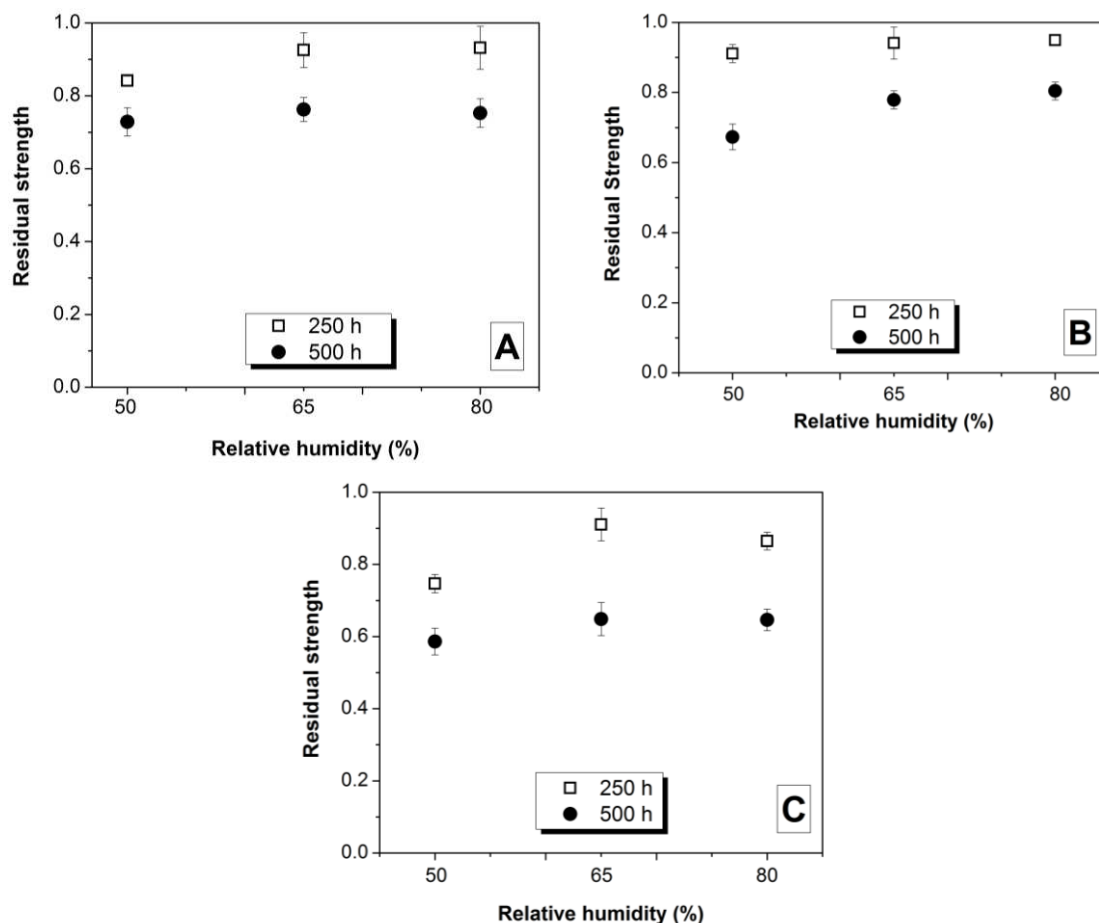
283

284 3.1.2. Residual compressive strength

285

286 The residual compressive strength (Figure 2) represents the ratio of the strengths of the concretes
287 before and after exposure to CO₂, providing a direct means of comparison of the samples which had
288 different strengths before carbonation (GBFS/(GBFS+MK) = 1.0: 63 MPa; GBFS/(GBFS+MK) = 0.9:
289 73 MPa; and GBFS/(GBFS+MK) = 0.8: 53 MPa). Concretes based solely on GBFS (Figure 2A) and
290 with GBFS/(GBFS+MK) = 0.9 (Figure 2B) show, over the first 250 h of exposure, only slight
291 reductions in the compressive strength relative to the uncarbonated concretes at relative humidities of

292 65% and 80%, while specimens exposed at an RH of 50% exhibit a reduction in the compressive
293 strength of around 15%. Similar trends are visible for specimens exposed for longer periods of time
294 (500 h), although the extent of strength loss increases notably with time. The effect of RH on the
295 carbonation progress of the concretes assessed seems to be more significant with the inclusion of MK
296 in the binder.
297



298 **Figure 2.** Residual compressive strengths of partially accelerated-carbonated concretes based on
299 alkali-activated slag/metakaolin blends formulated with GBFS/(GBFS+MK) ratios of (A) 1.0, (B) 0.9
300 and (C) 0.8, as a function of the relative humidity, at 1% CO₂. Error bars correspond to one standard
301 deviation of three measurements.

302
303 In a previous study where carbonation of some of these mix designs was studied at a single RH (65%)
304 for up to 1000 h [30], the correlation between carbonation depth and residual strength was observed to
305 be approximately linear for the concretes containing no more than 10% MK (GBFS/(GBFS+MK) \geq
306 0.9). However, such a relationship is not evident across the different RH values when comparing
307 Figures 1 and 2, particularly for the samples containing MK. The samples with GBFS/(GBFS+MK) =
308 0.9 exposed at 50% RH showed almost no additional carbonation depth (Figure 1B), but a marked
309 loss of strength (Figure 2B), between 250-500 h of exposure. The same mix exposed at 80% RH

310 showed a relatively rapid progression of the carbonation front, but almost no change in compressive
311 strength, between 250-500 h. However, the main disagreement between the carbonation depth and
312 carbonation rate data is visible when comparing the influence of RH on these two parameters: in each
313 case, 65% RH leads to the highest carbonation depth after 250 h of exposure, but the highest residual
314 strength after the same exposure time. The samples with GBFS/(GBFS+MK) = 0.8 are most deeply
315 carbonated, and lose the most strength, after 500h at 50% RH, but agreement between the conditions
316 which cause the greatest extent of damage as determined by these two different measures is not
317 observed for the concretes with GBFS/(GBFS+MK) = 0.9 or 1.0.

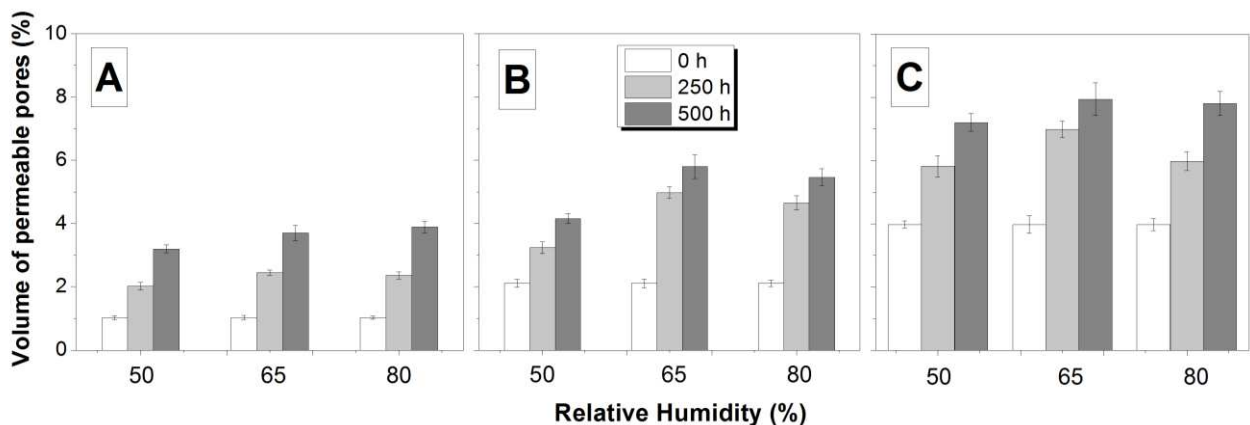
318

319 3.1.3. Total porosity and absorption

320

321 The carbonation of alkali-activated concretes leads to an increase in the volume of permeable pores
322 (Figure 3) so that the volume of permeable voids of carbonated specimens is twice the porosity of
323 uncarbonated samples, when the porosity of the sample as a whole is measured; considering the fact
324 that there is an undamaged core in most of the cylinders tested, this change may even be more notable
325 if solely the carbonated part of the sample were to be considered. This increase in porosity is in
326 general slightly greater when carbonation is carried out at increased relative humidities, but the
327 differences between different RH values are not highly significant.

328



329

330 **Figure 3.** Porosity of partially carbonated concretes based on alkali-activated slag/metakaolin blends
331 formulated with GBFS/(GBFS+MK) ratios of (A) 1.0, (B) 0.9 and (C) 0.8, as a function of the relative
332 humidity, at 1% CO₂. Error bars correspond to one standard deviation of four measurements
333

334

335 Increased porosity is exhibited by concretes exposed to CO₂ over longer times, as expected with
336 reference to the progress of the carbonation reaction in the material. Mixes with GBFS/(GBFS+MK)
337 = 0.8 show the highest total porosity of the specimens studied, which might contribute to the higher
338 carbonation rate identified in these concretes after 250 h of exposure compared with the systems

338 including lower contents of MK. In this case, the samples exposed at 65% RH show the largest
 339 increment in total porosity after 250 h of exposure; however, comparable porosities can be observed
 340 after 500 h when the exposure to CO₂ is conducted at 65% or 80% RH.

341
 342 These results agree reasonably well with the trends in carbonation depth as a function of relative
 343 humidity (Figure 1C), but disagree with the residual compressive strength data obtained for these
 344 specimens, where the lowest residual strengths were reported when the exposure was conducted at
 345 50% RH (Figure 2C). It is thus suggested that the different protocols for assessing the progress and
 346 influence of carbonation on an alkali-activated concrete are influenced in different ways by the
 347 relative humidity conditions under which the test is conducted, and this is likely to be very important
 348 when comparing data across different investigations, where various parameters are assessed under
 349 different conditions. This means that different trends will be obtained, depending on which
 350 performance parameters are selected for analysis.

351
 352 Total water absorption values for the concretes assessed are shown in Table 2, and it can be seen that
 353 although the influence of exposure RH on water absorption (as measured by the ASTM C642 test) is
 354 relatively minor, higher absorptions are generally observed in concretes with MK in the binder when
 355 exposed to carbonation at 65% RH, especially at longer times of exposure. It has been reported that,
 356 for conventional Portland cement-based concretes [36], absorption values of 3% and total porosity
 357 values of 10% are able to be related to concretes with good durability. Based on this, it is possible to
 358 suggest that all the concretes assessed here, both before and after CO₂ exposure, have the potential to
 359 be highly durable.

360
 361 **Table 2.** Water absorption (wt.%) of concretes based on alkali-activated GBFS/MK blends exposed to
 362 CO₂ under different relative humidities

GBFS/(GBFS+MK)	Relative humidity (%)	Time of exposure to CO ₂ (hours)		
		0	250	500
1.0	50		1.27	1.53
	65	0.28	0.99	1.27
	80		1.20	1.32
0.9	50		2.09	2.15
	65	0.58	2.16	2.29
	80		2.10	2.30
0.8	50		2.68	2.98
	65	1.38	2.95	3.11
	80		2.73	2.99

363
 364

365 As CO₂ can diffuse through both large and capillary pores, the total porosity is not the only factor that
366 can determine the progress of carbonation in alkali-activated concretes. For the mixes assessed here, it
367 has been observed when applying the standard procedure EMPA – SIA 162/1 [31] to study the
368 capillary uptake of water into a dried sample, that before carbonation the concretes present similar
369 resistance to water penetration ($\sim 1 \times 10^7$ s/m²) [30]. This parameter is one of the main coefficients
370 describing the capillary sorptivity of these materials, and provides information regarding the geometry
371 of the pore network of the assessed samples, where a higher resistance to water penetration indicates a
372 more tortuous pore structure hindering mass transport through the material. The fact that similar
373 values of resistance to water penetration are obtained across the concrete mixes studied indicates that
374 these materials present approximately comparable pore structures. Consequently, the differences in
375 the rates of carbonation at early stages of reaction of the mixes assessed are more likely to be
376 associated with the carbonation starting in the capillary pores, increasing the pore size (as previously
377 identified in alkali-activated mortars [9-10]), and thus diminishing the effect of the different quantities
378 of water present at different RH values.

379

380 **3.2. Effect of the CO₂ concentration on the carbonation of concretes based on activated** 381 **GBFS/MK blends**

382

383 Results reported in a previous study [22] show that accelerated carbonation induced in the pore
384 solutions of alkali-activated binders under different CO₂ concentrations promotes the formation of
385 different carbonation products, depending on both the CO₂ concentration and the temperature of the
386 test. This indicates that increased partial pressures of CO₂ shift the reaction equilibrium expected
387 under natural carbonation conditions, and therefore promote mechanisms which may lead to
388 disproportionately faster degradation of the material compared to what is likely to occur in actual
389 service. Thus, conflicting results could be obtained if the carbonation progress in alkali-activated
390 concretes is tested under different CO₂ exposure conditions, and this issue is examined in detail in the
391 following section. All the tests described in this section are conducted at 65% RH.

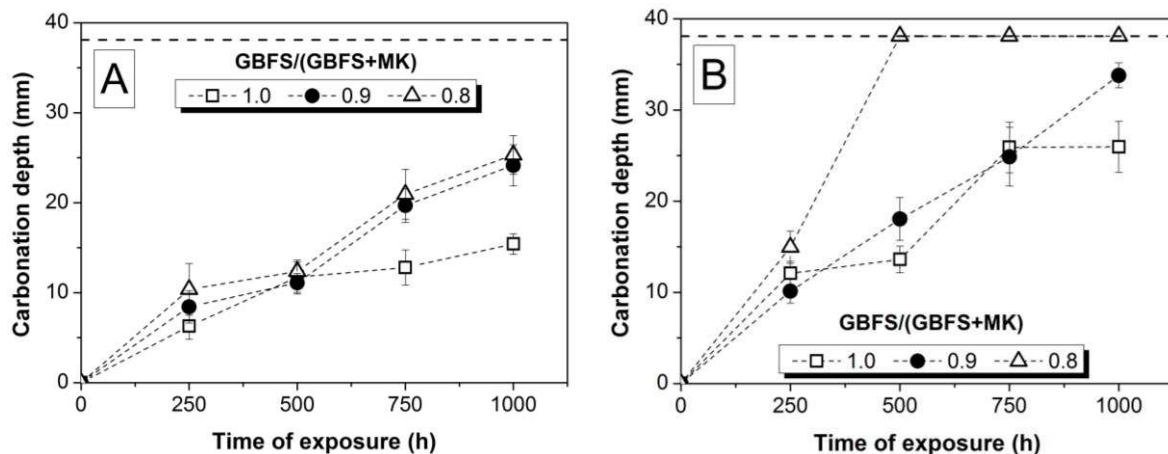
392

393 **3.2.1. Carbonation rate**

394

395 As discussed in detail in section 3.1 above, concretes exposed to 1% CO₂ (Figure 4A) show a higher
396 carbonation extent at increased contents of MK in the binder; however, the difference between
397 GBFS/(GBFS+MK) ratios of 0.8 and 0.9 is in general minor, while there is a notable difference
398 between the concretes with and without MK. Increasing the CO₂ concentration to 3% (Figure 4B)
399 promotes much faster carbonation of the specimens, as expected. However, its effect is more
400 detrimental in the concretes with GBFS/(GBFS+MK) = 0.8 than with GBFS/(GBFS+MK) = 0.9 or

401 1.0. This indicates that 3% CO₂ is too high a concentration of CO₂ to enable reliable prediction of the
402 in-service carbonation performance of alkali-activated concretes with different binder mix designs, as
403 it may not be possible to distinguish which differences are due to actual better or worse carbonation
404 resistance of the samples, and which are due to differences in the aggressiveness of the test towards
405 different binder chemistries. This is an important point, and further discussion is required to determine
406 the reasons for this behaviour.
407



408
409 **Figure 4.** Accelerated carbonation progress of alkali-activated slag/metakaolin blended concretes
410 induced at (A) 1% CO₂ and (B) 3% CO₂, and 65% RH. The horizontal dashed line in each plot
411 represents full carbonation of the cylindrical specimens used in the tests. Each value is the average of
412 20 measurements taken from two specimens. Error bars correspond to one standard deviation.
413

414 After 250 h of exposure, the concretes with GBFS/(GBFS+MK) = 0.8 show the highest carbonation
415 depths, consistent with the greater volume of permeable pores determined in these specimens before
416 testing, when compared with the concretes with GBFS/(GBFS+MK) = 0.9 or 1.0. At longer times of
417 exposure, the carbonation rates of concretes with GBFS/(GBFS+MK) = 0.9 or 1.0 remain comparable
418 when exposed to 3% CO₂ (Figure 4B), although there was a notable difference between these
419 specimens at 1% CO₂ (Figure 4A). When including 20% MK in the binder (GBFS/(GBFS+MK) =
420 0.8) and exposing the material to 3% CO₂, the carbonation progresses so rapidly that the concrete
421 specimens tested here (38.1 mm radius cylinders) are completely carbonated after only 500 h of
422 exposure.
423

424 This, combined with the porosity data in Figure 3 and in reference [30], indicates that concretes
425 presenting a higher volume of permeable pores before testing will be more aggressively subject to
426 carbonation penetration at higher CO₂ concentrations than would be expected when the material is
427 exposed to more moderate CO₂ concentrations. It is noted that 3% CO₂ is actually not a particularly

428 high concentration for use in an accelerated carbonation test for Portland cement systems.
429 Concentrations far exceeding this value (and even up to 100%) are widely used in international testing
430 programs for Portland cement concretes [28], although there has been limited systematic study of the
431 influence of these parameters on the chemistry of non-traditional cements and concretes [37]. This
432 strong dependence on CO₂ concentration when comparing binder types may also provide misleading
433 conclusions about the ‘real’ quality of the material in service, considering that alkali-activated
434 concretes often exhibit a substantial reduction in permeability at advanced ages of curing, and
435 therefore will behave differently if they are assessed at more mature ages [30].

436

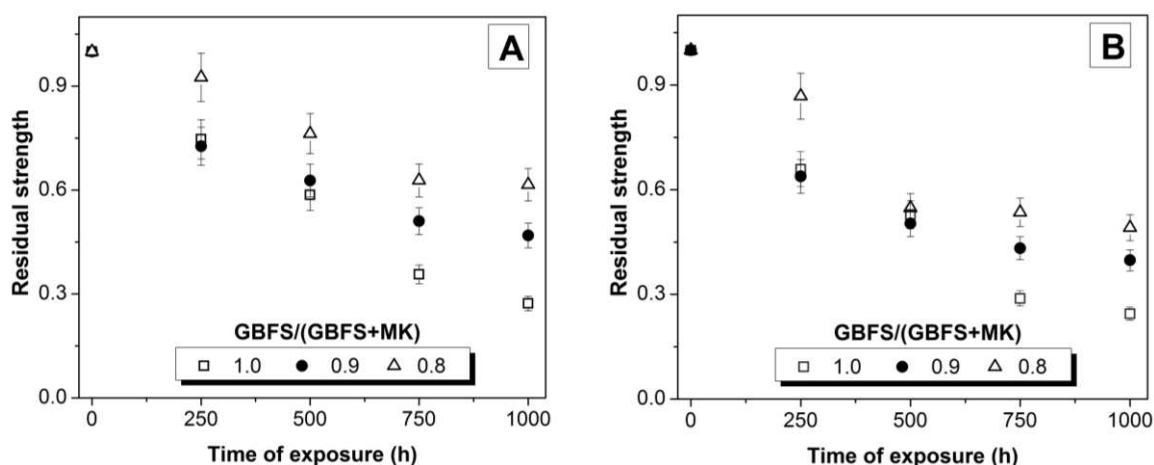
437

438 3.2.2. Residual mechanical strength

439

440 Residual mechanical strengths of specimens carbonated under 1% and 3% CO₂ environments are
441 shown in Figure 5. These results show that decreases in the compressive strength are induced as
442 consequence of the carbonation of the specimens, and that this is not strongly dependent on the
443 concentration of CO₂ exposure. The concretes including MK as a secondary binder component show
444 very little effect of CO₂ concentration on residual strength, while the slag-only binders show slightly
445 more loss of strength at 3% CO₂ than at 1%. However, although some samples revealed complete
446 carbonation when determined using the phenolphthalein indicator (Figure 4B; samples with
447 GBFS/(GBFS+MK) = 0.8 at 3% CO₂), the remnant compressive strength of those concretes (Figure
448 5B) is comparable with what is obtained in specimens of the same mix design carbonated at 1% CO₂
449 (Figure 5A), where these specimens showed only partial carbonation when carbonation depth was
450 determined using the same methodology.

451



452

453 **Figure 5.** Effect of the CO₂ concentration of exposure on the residual compressive strength of
454 partially carbonated concretes based on alkali-activated slag/metakaolin blends, exposed to

455 carbonation at (A) 1% or (B) 3% CO₂, and 65% RH. Error bars correspond to one standard deviation
456 of three measurements.

457

458 It therefore becomes evident that there is not a direct correlation between the degree of ingress of the
459 carbonation front, as identified using the phenolphthalein indicator, and the degree of degradation of
460 the material as measured by residual mechanical strength. If complete carbonation of the matrix was
461 taking place in these systems, the loss of loading capacity should be approximately proportional to the
462 loss of undamaged cross-section area, considering that carbonation is usually assumed to be
463 associated with the decalcification of the C-A-S-H gel formed during the activation of the slag [20].
464 However, ongoing reduction in the compressive strength with CO₂ exposure is identified in the
465 specimens with GBFS/(GBFS+MK) = 0.8, which were apparently completely carbonated (according
466 to the phenolphthalein test) within the first 250 h of exposure. This highlights the fact that carbonation
467 in alkali-activated binders cannot be understood solely as taking place via either pore solution effects,
468 or by the decalcification of the solid binder phases, but rather that both stages of the interaction
469 between CO₂ and the binder components (liquid and solid) must be considered.

470

471 The chemical reactions controlling the extent of carbonation in alkali-activated materials involve the
472 carbonation of the highly alkaline pore solution, and subsequently carbonation of secondary products
473 such as layered double hydroxides (i.e. hydrotalcite) and decalcification of C-A-S-H type products
474 [22]. Recent work [22] has shown that under accelerated carbonation conditions, the pore solution pH
475 in alkali activated binders is highly dependent on the partial pressure of CO₂, so that a decrease in the
476 pH to values below 10 could only be expected at CO₂ partial pressures higher than ambient, as the
477 pore solution chemistry changes from carbonate-dominated to bicarbonate-dominated. Considering
478 that the phenolphthalein indicator used here shows a colour change at pH values between 8.2 and 10
479 [38], it is likely that the colourless area observed in the carbonation testing is more likely to represent
480 the carbonation of the pore solution, rather than rather than the potential extent of degradation of the
481 C-A-S-H type phases in the binder matrix.

482

483 This is consistent with the fact that the concretes exposed to different CO₂ concentrations present
484 comparable compressive strengths, and that those showing complete carbonation within the first 250 h
485 of exposure report ongoing changes in residual strength after longer times of exposure to CO₂. These
486 later changes in compressive strength are associated with ongoing decalcification processes in the
487 binder, which take place after the local pH has decreased sufficiently to cause phenolphthalein to
488 remain colourless when sprayed onto the samples. It is entirely possible that there is also some
489 decalcification taking place simultaneously at the reaction front where the pH is decreasing, and this
490 will cause the start of the strength loss, but this is seen to continue long after the ‘carbonation front’

491 has passed, showing that the traditional conceptual model of this process taking place at a sharp
492 reaction front in Portland cement systems [39] is not appropriate for the systems studied here. It is
493 noted that some authors have also observed a multi-stage process in Portland cement carbonation, e.g.
494 [40], but the details of the mechanisms are likely to be very different in these specimens which do not
495 contain portlandite.

496

497

498 3.2.3. Water absorption properties

499

500 Given this apparent disconnect between measured carbonation depths and gel decalcification during
501 accelerated carbonation testing of alkali-activated binders, it thus appears valuable to analyse
502 alternative methods by which the progress and effects of the actual decalcification process can be
503 easily determined in an engineering sense, and it is likely that changes in the gel microstructure and
504 pore structure will provide useful information in this regard. Water absorption is a relatively
505 straightforward, although in many cases very sensitive and subtle, means of examining changes in
506 pore network structure. In this section, the effects of inducing carbonation at different CO₂ partial
507 pressures on the water absorption parameters of alkali-activated concretes are assessed.

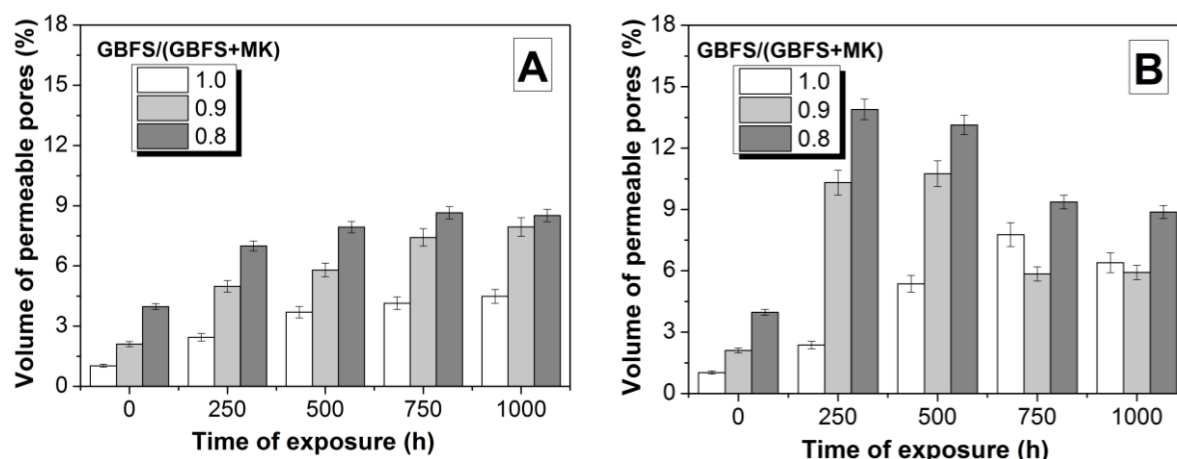
508

- 509 • Volume of permeable pores (ASTM C 642)

510

511 Concretes based solely on GBFS present the lowest volume of permeable pores among the concretes
512 studied prior to carbonation (Figure 6), and an increased volume of pores is identified with the
513 inclusion of higher contents of MK in the binder. This might be an intrinsic property of the more MK-
514 rich binders, but may also be related to the reduced workability identified in these concretes, which
515 makes moulding and compaction of the specimens more difficult. Exposure to 1% CO₂ (Figure 6A)
516 induces a gradual increment in the volume of permeable pores of the specimens throughout the time
517 of exposure, and a very consistent trend in this parameter is observed across the different binder
518 formulations. These results and trends differ from what is usually identified in Portland cement-based
519 materials, where the porosity is generally reduced by carbonation, along with a decrease in the content
520 of small radius pores due to pore blocking by carbonate reaction products [10].

521



522
523 **Figure 6.** Volume of permeable pores of accelerated carbonated concretes based on alkali-activated
524 slag/metakaolin blends exposed to (A) 1% and (B) 3% CO₂, at 65% RH. Each value is the average of
525 four measurements. Error bars correspond to one standard deviation.

526
527 However, an entirely different trend in the variations of the volume of permeable pores is identified in
528 alkali-activated concretes subjected to accelerated carbonation at 3% CO₂ (Figure 6B). Concretes
529 based solely on GBFS show a gradual increase in porosity during the first 750 h of exposure under
530 these conditions, consistent with the trend identified in these specimens at 1% CO₂ (Figure 6A), but
531 then a decrease in porosity after this time. The concretes with MK in the binder start from a slightly
532 higher porosity, but with exposure to 3% CO₂ show a very substantial increment in their porosity up
533 to 250 h (with GBFS/(GBFS+MK) = 0.8) or 500 h (with GBFS/(GBFS+MK) = 0.9), followed by a
534 significant reduction in porosity up to 1000 h of exposure. These results do not correlate well with the
535 observations related to carbonation front progress or residual compressive strength, where samples
536 with GBFS/(GBFS+MK) = 0.8 were apparently fully carbonated after 250 h of exposure to the same
537 CO₂ concentration, and the variations in strength (Figure 5B) were all monotonic rather than showing
538 any inflection points. It is currently unclear why the samples show a maximum in pore volume after
539 an intermediate duration of carbonation, as this would not logically be expected based on the current
540 understanding of the carbonation mechanisms in these systems, and this issue is identified as being
541 worthy of further analysis as a key part of the future development of reliable carbonation testing
542 protocols for alkali-activated concretes.

543
544 This behaviour provides further evidence that the use of increased concentrations of CO₂ to induce
545 carbonation of alkali-activated concretes leads to unrepresentative, and thus undesirable, changes in
546 the structure and chemistry of alkali-activated binders at early times of CO₂ exposure. This leads to a
547 faster reduction of the pH in the pore solution of the sample, decreasing into the phenolphthalein
548 colour change range, than what would be expected under natural carbonation conditions, and therefore

549 the identification of a ‘false’ carbonation. Consistent with this is the fact that there are ongoing
550 changes in the strength and permeability of ‘completely’ carbonated specimens, as a consequence of
551 reactions that continue taking place over time. This also agrees with the observation that reductions in
552 the volume of permeable pores are observed here as a consequence of the deposition of solid
553 carbonation products, which appear to contribute to the plugging of some of the additional pores
554 formed during carbonation.

555

556 • Capillary sorptivity

557

558 The degradation of reinforced concrete under CO₂ exposure involves both the carbonation of the
559 matrix, leading to a reduction of the alkalinity of the system, and the consequent depassivation of the
560 steel rebars, which makes them susceptible to a series of corrosive attacks such as pitting, which is
561 accelerated by the presence of chloride and is extremely harmful for the integrity of the concrete
562 structure as a whole. It has been reported [41] that similar to the situation for Portland cement based
563 materials, the ingress of chlorine anions into alkali-activated concretes takes place through the
564 capillary pores. Several studies agree [30, 33, 42, 43] that uncarbonated alkali-activated mortars and
565 concretes present low capillary sorptivity, and consequently a high resistance to chloride penetration,
566 when compared with conventional Portland cement concretes; however, the changes in the capillary
567 sorptivity of these concretes induced by carbonation have not previously been studied in detail.

568

569 The exposure to 1% CO₂ of concretes based solely on GBFS (Figure 7A) for 250 h leads to a
570 substantial increment in the total capillary water uptake of the material, which is higher by as much as
571 a factor of 3 than in uncarbonated specimens. However, this dramatic increase is only temporary, and
572 the exposure of these samples to 1% CO₂ for longer periods of times then brings the amount of
573 absorbed water down to be similar to the unexposed material after 750 h of exposure to 1% CO₂. The
574 same is true for the samples with GBFS/(GBFS+MK) = 0.9 (Figure 7B). This indicates that partial
575 carbonation of the specimens may inhibit the ingress of aggressive agents such as chlorides into the
576 concrete, but that the complete carbonation of alkali-activated concretes after this time leads to
577 reductions in the capillarity as a consequence of the precipitation of carbonation products. This time-
578 dependent behaviour was not observed in any other material parameters analysed during exposure to
579 1% CO₂, but shows some subtle effects in changes in pore size distribution which were not observed
580 in the overall porosity data.

581

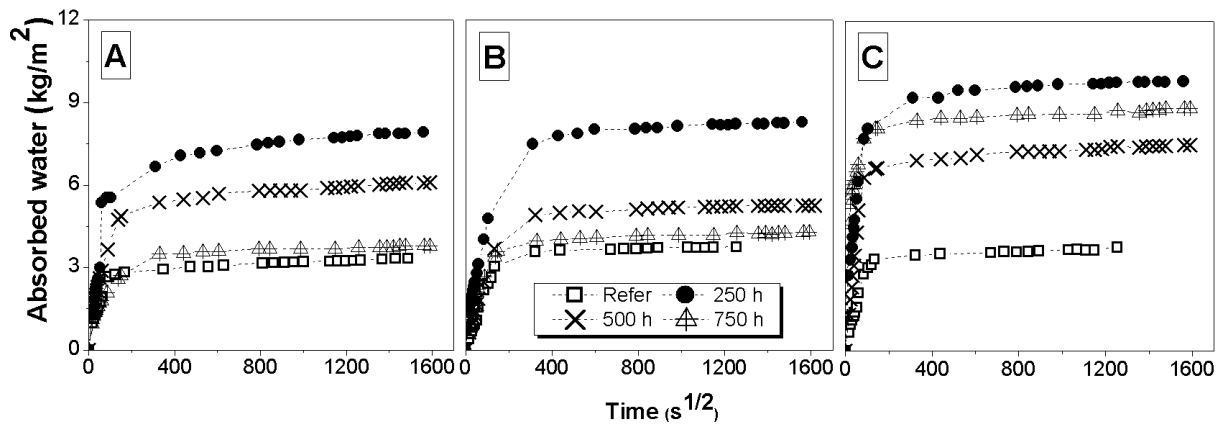


Figure 7. Capillary sorptivity curves of accelerated carbonated concretes based on alkali-activated slag/metakaolin blends formulated with GBFS/(GBFS+MK) ratios of (A) 1.0, (B) 0.9 and (C) 0.8, exposed to 1% CO₂ at 65% RH.

However, concretes formulated with GBFS/(GBFS+MK) = 0.8 (Figure 7C) do not display such a notable reduction in the capillary suction with the progress of carbonation in the specimens. The total water absorbed by the samples exposed to 1% CO₂ for 750 h is almost as high as after 250 h of exposure, and almost three times as high as the water uptake of the unexposed material. This may be associated with the lower Ca content of the gel in this mix, leading to the formation of less solid carbonation products to plug the pores in the material, or may be attributed to factors related to shrinkage and/or microcracking in the gel, which is also likely to be changed by the differences in Ca and Al content as a function of MK addition [29, 30].

Concretes carbonated at a CO₂ concentration of 3% (Figure 8) display water saturation after a shorter period of time than similar concretes carbonated at 1% CO₂ (Figure 7). Concretes exposed to 3% CO₂ for 250 h again show a marked increase in capillary water uptake compared with uncarbonated specimens. After 500 h of exposure (Figure 8A), a substantial reduction in water uptake is identified in specimens based solely on GBFS; however, exposure to this CO₂ concentration for longer periods of time leads again to increments in the amount of absorbed water compared with those identified after 250 h, and the water uptake after 1000 h of carbonation is approximately double the uptake of the unexposed concretes.

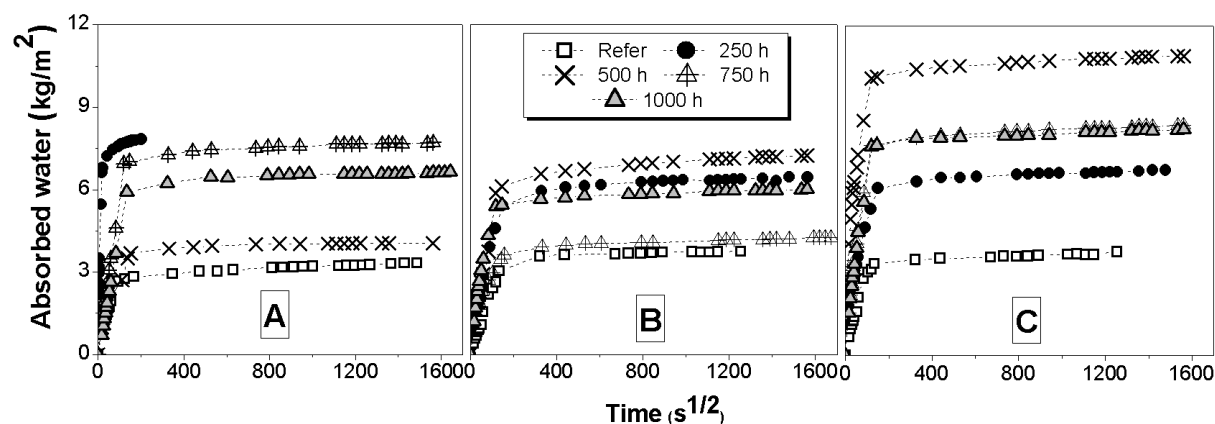


Figure 8. Capillary sorptivity curves of accelerated carbonated concretes based on activated slag/metakaolin blends formulated with GBFS/(GBFS+MK) ratios of (A) 1.0, (B) 0.9 and (C) 0.8, exposed to 3% CO₂ at 65% RH.

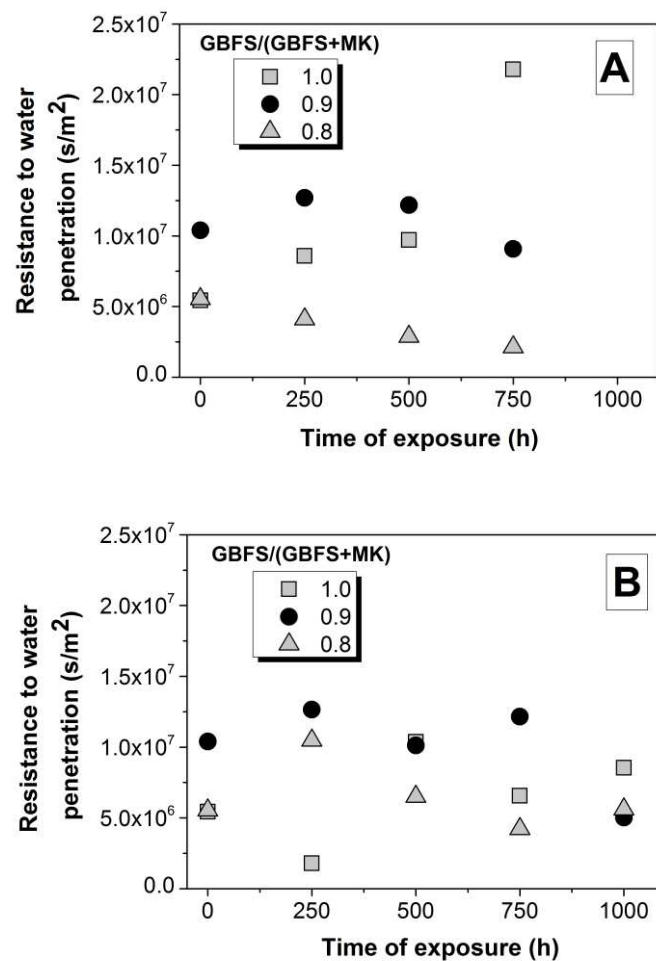
In concretes formulated with GBFS/(GBFS+MK) = 0.9 (Figure 8B), a similar trend is observed, with a reduction in absorbed water after 750 h of exposure but an increased permeability observed at the other times of exposure. This differs from the observations for these concretes when exposed to 1% CO₂, where reductions in the capillary permeability at extended periods of exposure were observed (Figure 7B). This again demonstrates that exposure of alkali-activated concretes to different CO₂ concentrations promotes the development of different pore structures, and therefore variations in the transport of CO₂ inside the material, which can give potentially misleading indications regarding the carbonation performance which would be identified in service in these concretes.

Increasing the MK content of the binder to 20% (GBFS/(GBFS+MK) = 0.8) again leads to increased water absorption at extended times of CO₂ exposure (Figure 8C). This is consistent with the high total porosity observed in these specimens when compared with concretes with lower contents of MK. In this case, similar behaviour is observed at 1% and 3% CO₂ – which may mean either that both of these testing conditions are appropriate for the analysis of these concretes, or that even 1% CO₂ is too high a concentration to provide a good representation of the performance of the concretes in service. At this point it is not possible to say which of these possibilities is more likely, but the effect of elevated CO₂ concentrations on pore solution chemistry [22] indicates that the concentrations are probably too high to fully accurately represent the in-service carbonation of alkali-activated concretes, even at these levels which are quite moderate by the standards of most carbonation tests [28].

The kinetics of the capillary sorption of water into concrete can be described by the resistance to

water penetration ($m = \frac{\text{saturation time}}{(\text{penetration depth})^2}$). The values of this parameter, as determined from

632 capillary sorption curves of concretes exposed to 1% CO₂ (Figure 7) and 3% CO₂ (Figure 8), are
633 shown in Figure 9. Concretes exposed to 1% CO₂ display lower resistance to water penetration at
634 extended periods of exposure, which is consistent with the increased volume of permeable pores
635 observed in those concretes (Figure 6). On the other hand, for concretes exposed to 3% CO₂, the
636 fluctuations in the m values are approximately consistent with the total porosity of these concretes,
637 indicating the high variability of capillary pore structure induced during carbonation at such a high
638 CO₂ concentration.
639



640 **Figure 9.** Resistance to water penetration (m) of carbonated alkali-activated concretes exposed at 65%
641 RH, and (A) 1% CO₂ or (B) 3% CO₂, for durations as marked.

642
643
644
645
646
647

4. Conclusions

The key outcome of this study is the observation that accelerated carbonation testing of alkali-activated concretes depends strongly on both the testing conditions and the chemistry of the binder. The inclusion of more than 10% MK ($\text{GBFS}/(\text{GBFS}+\text{MK}) < 0.9$) in activated-slag binders leads to notably increased carbonation rate and extent, as these specimens develop increased permeability. The performance of samples with $\text{GBFS}/(\text{GBFS}+\text{MK}) = 0.9$ or 1.0 is sometimes similar, or sometimes the samples with $\text{GBFS}/(\text{GBFS}+\text{MK}) = 0.9$ carbonate more rapidly, depending on the test conditions. In the relative humidity range tested (50-80%), the highest carbonation rates are generally observed in specimens exposed at a relative humidity of $65\pm 5\%$, indicating that a partially saturated moisture condition accelerates the carbonation reaction process. For carbonation tests where the specimens were not dried prior to testing, the water absorption of the uncarbonated samples provides a good indication of whether drying effects during the test duration will retard the initial stages of carbonation. Testing samples with low water absorption (i.e. initially highly saturated and refined pore networks) at high relative humidity gives a very low carbonation rate in the early stages of the test, as the carbonation of the saturated binder is slow, followed by an acceleration of the carbonation process as the drying front begins to enter the sample to a more significant extent.

The progress of carbonation in alkali-activated concretes is also very strongly dependent on the CO_2 concentration used during the accelerated testing, as differences in the total porosity and mainly in the capillary pore structure are induced at higher CO_2 concentrations. At relatively low CO_2 concentration (1%), a monotonic increase in porosity, along with an eventual reduction in capillarity, can be identified in the concretes assessed, indicating that the formation of carbonation products in these systems is contributing to changes in the pore network structure during the test. On the other hand, carbonation induced at higher CO_2 concentrations (3%) shows less clarity in the relationships between measured carbonation depth, residual strength and porosity.

Concretes which appear fully carbonated after only 250 h of testing when the pH is revealed by a phenolphthalein indicator continue to show structural changes over 1000 h, showing that there are likely to be multiple steps in the carbonation process (most probably carbonation of the alkali-rich pore solution in the first instance, followed by later decalcification of the gel), and that the phenolphthalein method shows only the progress of the first of these processes. The rates of pore solution carbonation and gel carbonation seem to be particularly distinct from each other at higher CO_2 concentration, meaning that such test conditions lead to the prediction of poor performance in alkali-activated concretes, which may not accurately represent the behaviour of the materials under exposure to natural carbonation. It is therefore not recommended to carry out accelerated carbonation

684 testing of alkali-activated binders at CO₂ concentrations higher than 1% CO₂. The results obtained
685 from these experiments are more an indication of the loss of alkalinity in these materials due to pore
686 solution chemistry (which is highly subject to differences in CO₂ partial pressure), rather than the
687 degradation due to decalcification of the binding gel, and it cannot be considered as a sole predictor of
688 their durability.

689

690 Finally, it is noted that the interaction between carbonation and drying in alkali-activated concretes
691 certainly requires further investigation – there is a coupling effect whereby drying influences
692 carbonation, and carbonation influences drying, and the study of these effects in parallel in a
693 laboratory (or field) setting has not yet been fully developed. This is an area requiring further
694 research, as highlighted by the fact that this paper has opened almost as many questions as it has
695 answered in this area.

696

697

698 **Acknowledgements**

699

700 This study was sponsored by Universidad del Valle (Colombia), the Center of Excellence of Novel
701 Materials (CENM) and Patrimonio Autónomo Fondo Nacional de Financiamiento para la Ciencia, la
702 *Tecnología y la Innovación “Francisco José de Caldas” Contrato RC - No. 275-2011*. The
703 participation of S.A Bernal and J.L. Provis has been sponsored in part by the University of
704 Sheffield, and the research leading to these results has received funding from the European
705 Research Council under the European Union's Seventh Framework Programme (FP/2007-
706 2013) / ERC Grant Agreement #335928 (GeopolyConc). We would also like to thank the
707 anonymous reviewers for the extensive discussions which help to improve this paper.

708

709 **References**

710

- 711 1. Hobbs DW (2001) Concrete deterioration: causes, diagnosis, and minimising risk. *Int*
712 *Mater Rev* 46(3):117-144.
- 713 2. Basheer L, Kropp J, Cleland DJ (2001) Assessment of the durability of concrete from
714 its permeation properties: a review. *Constr Build Mater* 15:93-103.
- 715 3. Poonguzhali A, Shaikh H, Dayal RK, Khatak HS (2008) Degradation mechanism and
716 life estimation of civil structures – A review. *Corros Rev* 26(4):215-294.
- 717 4. Fernández-Bertos M, Simons SJR, Hills CD, Carey PJ (2004) A review of accelerated
718 carbonation technology in the treatment of cement-based materials and sequestration
719 of CO₂. *J Hazard Mater B* 112:193-205.
- 720 5. Bary B, Sellier A (2001) Coupled moisture—carbon dioxide—calcium transfer model
721 for carbonation of concrete. *Cem Concr Res* 34:1859-1872.

- 722 6. Živica V, Bajza A (2001) Acidic attack of cement based materials — a review: Part 1.
723 Principle of acidic attack. *Constr Build Mater* 15(8):331-340.
- 724 7. Johannesson B, Utgenannt P (2001) Microstructural changes caused by carbonation of
725 cement mortar. *Cem Concr Res* 31:925-931.
- 726 8. Papadakis VG, Vayenas CG, Fardis MN (1989) A reaction engineering approach to
727 the problem of concrete carbonation. *AIChE J* 35(10):1639-1650.
- 728 9. Papadakis VG, Vayenas CG, Fardis MN (1991) Experimental investigation and
729 mathematical modeling of the concrete carbonation problem. *Chem Eng Sci* 46:1333-
730 1338.
- 731 10. Houst YF, Wittmann FH (1994) Influence of porosity and water content on the
732 diffusivity of CO₂ and O₂ through hydrated cement paste. *Cem. Concr. Res.*
733 24(6):1165 - 1176.
- 734 11. Houst YF (1996) The role of moisture in the carbonation of cementitious materials.
735 *Int. Z. Bauinst.* 2(1):49 - 66.
- 736 12. Younsi A, Turcry P, Ait-Mokhtar A, Staquet S (2013) Accelerated carbonation of
737 concrete with high content of mineral additions: Effect of interactions between
738 hydration and drying. *Cem Concr Res* 43:25-33.
- 739 13. Deja J (2002) Carbonation aspects of alkali activated slag mortars and concretes. *Silic*
740 *Industr* 67(1):37-42.
- 741 14. Shi C, Krivenko PV, Roy DM. *Alkali-Activated Cements and Concretes*, Abingdon,
742 UK: Taylor & Francis, 2006.
- 743 15. Xu H, Provis JL, van Deventer JSJ, Krivenko PV (2008) Characterization of aged slag
744 concretes. *ACI Mater J* 105(2):131-139.
- 745 16. Bernal SA, San Nicolas R, Provis JL, Mejía de Gutiérrez R, van Deventer JSJ (2014)
746 Natural carbonation of aged alkali-activated slag concretes. *Mater Struct* DOI:
747 10.1617/s11527-013-0089-2.
- 748 17. Bernal SA, Mejía de Gutierrez R, Rose V, Provis JL (2010) Effect of silicate modulus
749 and metakaolin incorporation on the carbonation of alkali silicate-activated slags.
750 *Cem Concr Res* 40(6):898-907.
- 751 18. Puertas F, Palacios M, Vázquez T (2006) Carbonation process of alkali-activated slag
752 mortars. *J Mater Sci* 41:3071-3082.
- 753 19. Palacios M, Puertas F (2006) Effect of carbonation on alkali-activated slag paste. *J*
754 *Am Ceram Soc* 89(10):3211-3221.
- 755 20. Bernal SA, Provis JL, Walkley B, San Nicolas R, Gehman JD, Brice DG, Kilcullen A,
756 Duxson P, van Deventer JSJ (2013) Gel nanostructure in alkali-activated binders
757 based on slag and fly ash, and effects of accelerated carbonation. *Cem Concr Res*
758 53:127-144.
- 759 21. Bernal SA, San Nicolas R, Myers RJ, Mejía de Gutiérrez R, Puertas F, van Deventer
760 JSJ, Provis JL (2014) MgO content of slag controls phase evolution and structural
761 changes induced by accelerated carbonation in alkali-activated binders. *Cem Concr*
762 *Res* 57:33-43.
- 763 22. Bernal SA, Provis JL, Brice DG, Kilcullen A, Duxson P, van Deventer JSJ (2012)
764 Accelerated carbonation testing of alkali-activated binders significantly underestimate
765 the real service life: The role of the pore solution. *Cem Concr Res* 42(10):1317-1326.
- 766 23. Ismail I, Bernal SA, Provis JL, Hamdan S, van Deventer JSJ (2013) Drying-induced
767 changes in the structure of alkali-activated pastes. *J Mater Sci* 48:3566-3577.
- 768 24. Ishida T, Meakawa K, Soltani M (2004) Theoretically identified strong coupling of
769 carbonation rate and thermodynamic moisture states in micropores of concrete.
770 2(2):213 - 222.

- 771 25. EN 13295:2004: Products and systems for the protection and repair of concrete
772 structures – test methods – Determination of resistance to carbonation. .
- 773 26. Harrison TA, Jones MR, Newlands MD, Kandasami S, Khanna G (2012) Experience
774 of using the prTS 12390-12 accelerated carbonation test to assess the relative
775 performance of concrete. *Mag Concr Res* 64(8):737-747.
- 776 27. Sanjuán MA, Andrade C, Cheyreyzy M (2003) Concrete carbonation test in natural and
777 accelerated conditions. *Adv Cem Res* 15(4):171 - 180.
- 778 28. da Silva FG, Helene P, Castro-Borges P, Liborio JBL (2009) Sources of variations
779 when comparing concrete carbonation results. *J Mater Civ Eng* 21(7):333-342.
- 780 29. Bernal SA, Provis JL, Mejía de Gutierrez R, Rose V (2011) Evolution of binder
781 structure in sodium silicate-activated slag-metakaolin blends. *Cem Concr Compos*
782 33(1):46-54.
- 783 30. Bernal SA, Mejia de Gutierrez R, Provis JL (2012) Engineering and durability
784 properties of concretes based on alkali-activated granulated blast furnace
785 slag/metakaolin blends. *Constr Build Mater* 33:99-108.
- 786 31. Fagerlund G (1982) On the capillarity of concrete. *Nord Concr Res* 1:6.1-6.20.
- 787 32. Levenspiel O. *Chemical Reaction Engineering*, 3rd Ed., New York: Wiley, 1999.
- 788 33. Bernal SA, Mejía de Gutierrez R, Pedraza AL, Provis JL, Rodríguez ED, Delvasto S
789 (2011) Effect of binder content on the performance of alkali-activated slag concretes.
790 *Cem Concr Res* 41(1):1-8.
- 791 34. Roy SK, Poh KB, Northwood DO (1999) Durability of concrete—accelerated
792 carbonation and weathering studies. *Build. Environ.* 34(5):597-606.
- 793 35. El-Turki A, Ball RJ, Allen GC (2007) The influence of relative humidity on structural
794 and chemical changes during carbonation of hydraulic lime. *Cem. Concr. Res.*
795 37(8):1233-1240.
- 796 36. Collins F, Sanjayan JG (2000) Effect of pore size distribution on drying shrinking of
797 alkali-activated slag concrete. *Cem Concr Res* 30(9):1401-1406.
- 798 37. Hyvert N, Sellier A, Duprat F, Rougeau P, Francisco P (2010) Dependency of C–S–H
799 carbonation rate on CO₂ pressure to explain transition from accelerated tests to natural
800 carbonation. *Cem Concr Res* 40(11):1582-1589.
- 801 38. Vassie PR. Measurement techniques for the diagnosis, detection and rate estimation
802 of corrosion in concrete structures. In: Dhir RK, Newlands MD, eds. *Controlling
803 concrete degradation, Proceedings of the International Seminar*. Dundee, Scotland,
804 Thomas Telford, 1999. pp. 215-229.
- 805 39. Castellote M, Andrade C (2008) Modelling the carbonation of cementitious matrixes
806 by means of the unreacted-core model, UR-CORE. *Cem Concr Res* 38(12):1374-
807 1384.
- 808 40. Thierry M, Villain G, Dangla P, Platret G (2007) Investigation of the carbonation front
809 shape on cementitious materials: Effects of the chemical kinetics. *Cem Concr Res*
810 37(7):1047-1058.
- 811 41. Roy DM, Jiang W, Silsbee MR (2000) Chloride diffusion in ordinary, blended, and
812 alkali-activated cement pastes and its relation to other properties. *Cem Concr Res*
813 30:1879-1884.
- 814 42. Collins F, Sanjayan J (2010) Capillary shape: Influence on water transport within
815 unsaturated alkali activated slag concrete. *J Mater Civil Eng* 22(3):260-266.
- 816 43. Shi C (1996) Strength, pore structure and permeability of alkali-activated slag
817 mortars. *Cem Concr Res* 26(12):1789-1799.
- 818
- 819